Journal of Neural Engineering

PAPER

Amplitude versus spatially modulated electrotactile feedback for myoelectric control of two degrees of freedom

To cite this article: Martin A Garenfeld *et al* 2020 *J. Neural Eng.* **17** 046034

IOP Publishing J. Neural Eng. 17 (2020) 046034 https://doi.org/10.1088/1741-2552/aba4fd

Journal of Neural Engineering

CrossMark

RECEIVED
26 February 2020

REVISED
6 July 2020

ACCEPTED FOR PUBLICATION
10 July 2020

PUBLISHED
11 August 2020

PAPER

Amplitude versus spatially modulated electrotactile feedback for myoelectric control of two degrees of freedom

Martin A Garenfeld[1], **Christian K Mortensen**[1], **Matija Strbac**[2], **Jakob L Dideriksen**[1] and **Strahinja Dosen**[1]

[1] Department of Health Science and Technology, Aalborg University, Frederik Bajers Vej 7D, 9220, Aalborg Ø, Denmark
[2] Tecnalia Serbia Ltd., Deligradska 9/39, 11000, Belgrade, Serbia

E-mail: magar@hst.aau.dk and sdosen@hst.aau.dk

Keywords: closed-loop control, electrotactile stimulation, myoelectric prosthesis, proprioceptive feedback, sensory feedback

Abstract

Objective. Artificial proprioceptive feedback from a myoelectric prosthesis is an important aspect in enhancing embodiment and user satisfaction, possibly lowering the demand for visual attention while controlling a prosthesis in everyday tasks. Contemporary myoelectric prostheses are advanced mechatronic systems with multiple degrees of freedom, and therefore, to communicate the prosthesis state, the feedback interface needs to transmit several variables simultaneously. In the present study, two different configurations for conveying proprioceptive information of wrist rotation and hand aperture through multichannel electrotactile stimulation were developed and evaluated during online myoelectric control. *Approach.* Myoelectric recordings were acquired from the dominant forearm and electrotactile stimulation was delivered on the non-dominant forearm using a compact interface. The first feedback configuration, which was based on spatial coding, transmitted the information using a moving tactile stimulus, whereas the second, amplitude-based configuration conveyed the position via sensation intensity. Thirteen able-bodied subjects used pattern classification-based myoelectric control with both feedback configurations to accomplish a target-reaching task. *Main results.* High task performance (completion rate > 90%) was observed for both configurations, with no significant difference in completion rate, time to reach the target, distance error and path efficiency, respectively. *Significance.* Overall, the results demonstrated that both feedback configurations allowed subjects to perceive and interpret two feedback variables delivered simultaneously, despite using a compact stimulation interface. This is an encouraging result for the prospect of communicating the full state of a multifunctional hand prosthesis.

1. Introduction

The loss of an upper limb is a traumatic and life-changing event leading to a significantly reduced quality of life due to restrictions in function, sensation and appearance [1, 2]. In an effort to restore normal functionality, myoelectric prostheses of various complexity have been introduced to replace the missing limb [3]. However, despite advancements in prosthetic technologies about 25% of users choose to abandon their myoelectric prosthetic device [4]. In user reviews, different reasons for the low user satisfaction were listed, from limitations in ergonomics to problems in control robustness and dexterity [5]. The lack of exteroceptive and proprioceptive feedback is also often indicated as an important problem and future design goal [1, 6], and may contribute indirectly to suboptimal control. Specifically, without somatosensory feedback, the user must rely only on visual observations when controlling the prosthesis, which is cognitively taxing [7]. Therefore, closing the loop is expected to improve prosthesis utility and user experience. Indeed, several studies have found that providing tactile stimulation through substitution feedback interfaces can improve user performance [8–12]. However, only one commercially available prosthesis (VINCENT evolution 2, Vincent Systems Gmbh, Germany), provides the user with feedback information about grasping force using a single vibrotactile motor [13].

Some techniques for restoring somatosensory feedback can elicit somatotopic sensations; i.e. they are felt as emanating from the phantom limb, which presumably enables more intuitive interpretation [14]. Although this can be achieved to some degree via transcutaneous electrical nerve stimulation [15, 16], such feedback is typically implemented by electrically stimulating peripheral sensory nerves [17, 18] or somatosensory cortex in the brain [19, 20] using implanted electrodes. Since this activates the same neural structures that have been used before amputation, the elicited sensations can be felt as emanating from the phantom limb. Some amputees, however, can be reluctant to undergo additional invasive treatments due to associated risks of post-surgery complications [5]. Alternatively, the feedback can be restored using a method called sensory substitution [14]. This is a non-invasive approach in which sensor data from the prosthesis are transmitted to the user by delivering mechanical or electrical stimulation to the skin of his/her residual limb.

The two most common substitution feedback methods are vibrotactile and electrotactile stimulation [21, 22]. The former relies on miniature motors to generate vibrations that can be tangential or perpendicular to the skin, while the latter elicits tactile sensations by delivering low-intensity electrical pulses to activate skin afferents. Electrical stimulation can produce uncomfortable sensations if the parameters are not appropriately adjusted. However, it is also characterized by low power consumption, decoupled parameters, and compact electronics that can be customized in a wide range of configurations with a different number and arrangement of electrode pads [23]. To deliver feedback information, the prosthesis sensor data has to be translated into stimulation profiles by associating the sensor information to stimulation parameters and location [24]. With parameter modulation, a feedback variable is communicated by changing stimulation intensity and/or frequency, while with spatial coding the variable is conveyed by changing active electrode pads [25].

In most studies in the literature, feedback interfaces were designed to transmit a single feedback variable, most often the grasping force [14, 26]. Nevertheless, the users have also expressed an interest in receiving proprioceptive information [6]. The proprioceptive feedback is particularly important in the execution of movements without full visual attention [27]. Communicating proprioceptive information might lower the need for visual attention during prosthesis use, thereby decreasing the cognitive load [6]. Contrary to force feedback that was investigated in many studies (reviewed in [14, 26]), artificial proprioception was addressed in only few works using invasive [28, 29] and non-invasive [30, 31] methods.

Importantly, commercially available upper-limb prosthetic devices have multiple degrees of freedom (DoFs) [5]. A typical configuration is a gripper that can open and close, equipped with a wrist rotation unit. Therefore, to provide full information regarding the state of this system, hand aperture as well as wrist rotation angle need to be transmitted simultaneously.

The studies investigating the communication of more feedback variables have used different tactile displays [9, 10, 28, 32–34]. In [9] and [10], Witteveen *et al* transmitted the sensory feedback of grasping force and hand aperture through a single vibrator and an array of vibrotactile actuators, respectively. Schiefer *et al* [28] implemented the feedback of fingertip pressure and hand aperture delivered through peripheral nerve stimulation. Arakeri *et al* [33] provided information regarding grip force and hand aperture by modulating the amplitude of two independent electrode pairs located on the dorsal left and right side of the neck. In [34], D'Anna *et al* provided hand aperture and grip force information via amplitude modulated intraneural electrical stimulation.

Therefore, most of the previous studies relied on the parameter modulation via two stimulation channels to simultaneously communicate two feedback variables. The other coding schemes such as spatial modulation were not investigated (expect in [9, 10]) and more importantly, different encodings have not been compared in terms of effectiveness. The latter is particularly relevant considering that the compact solutions for multichannel tactile stimulation are becoming available (see [32]). Such systems, equipped with many channels and independently adjustable parameters, allow a great flexibility in designing stimulation patterns that can be modulated in time, parameter and space to communicate the feedback on multiple DoFs simultaneously.

In the present study, therefore, a compact electronic stimulator with 16 channels [32] was used to directly compare the performance of two novel stimulation schemes based on spatial and amplitude coding, respectively. The encodings were designed to convey simultaneous electrotactile proprioceptive feedback from two DoFs of a prosthesis, namely, wrist pronation/supination and hand aperture. In this case, the challenge is that the subject needs to independently perceive and interpret two electrotactile information channels that are delivered at the same time to the skin using a compact interface with closely spaced pads. The use of the simultaneous multi-DoF feedback was tested during online myoelectric control, which includes not only perception and interpretation of elicited sensations but also mapping of the feedback into appropriate command signals. The hypothesis was that the spatial modulation, communicating proprioceptive information by a moving stimulus, would perform better than the amplitude encoding since the former might be more intuitive and easier to discriminate.

2. Methods

The two feedback schemes were evaluated by integrating the electrotactile interface into a commonly used setup [35–39] for the assessment of online myoelectric control based on pattern classification and target reaching task.

2.1. Experimental setup

The experimental setup is shown in figure 1. For the recording of electromyographic (EMG) signals, the Myo Armband from Thalmic Labs was placed on the dominant forearm, approximately 5 cm distally from the elbow crease with the main module (signed with the logo) positioned in the middle of the dorsal side. The Myo Armband integrates eight dry, stainless-steel electrode channels that are equidistantly arranged around the circumference of the forearm. The armband was connected via a Bluetooth 4.0 unit to a standard desktop PC. Despite having a limited sample rate of 200 Hz, high classification accuracy for myoelectric control can be achieved [40]. This configuration of EMG electrodes has been commonly used for myoelectric control [41].

The electrode array used to deliver electrical stimulation is shown in figure 2. The electrode array consisted of a single elongated pad designated as a common reference electrode and 16 circular pads designated to act as active electrodes. The electrodes were made by screen-printing conductive Ag/AgCl and dielectric inks for biomedical applications over 150 μm thick PET film. All pads were covered with conductive hydrogel (AG725, Axelgaard, Denmark) to enhance skin-electrode contact. A compact multichannel stimulation device (MaxSens, Tecnalia, Spain) generating biphasic pulses was connected to the standard desktop PC via USB. The pulse width and amplitude could be modulated independently for each pad whereas the frequency was common to all pads. The pulse width could be adjusted within a 50–1000 μs range with 10 μs steps, frequency from 1–400 Hz with 1 Hz steps and current amplitude from 50–10 000 μA with 0.1 μA steps. The electrode array was designed to provide feedback on the forearm [25, 32, 42], and it can be placed either longitudinally or transversely. A recent study has shown that there was no substantial difference between the two arrangements [43], and therefore, the circumferential placement was selected in the present setup because it is more compact. The electrode was wrapped around the non-dominant arm of the participant (figure 1) to avoid contaminating the recorded EMG [44, 45]. It was fitted such that the end pads had a maximum gap of 3 cm centrally on the volar side. Hence, the distal location of the electrode array depended on the circumference of the subject's forearm. This positioning strategy was applied to assure that the electrode covered as much of the circumference as possible. Therefore, the stimulation could be delivered to both sides of the arm with no spatial overlap between the most distal pads. The electrode connector (figure 2) was aligned with the axis of the forearm and positioned along the middle of the dorsal side. The electrode was strapped by an elastic sport band and the stimulator was attached to the top of the band (figure 1).

The subject was seated in a comfortable chair. During the experiment, the non-dominant hand was placed on the table and the dominant hand was held vertically relaxed by the side of the body. A 22" monitor was positioned on the table approximately 50 cm from the subject. The monitor was used to provide visual feedback when required (see *2.4.*). The desktop PC received recorded EMG and controlled stimulation parameters. The online control loop was programmed in Matlab 2018b (MathWorks, USA).

2.2. Myoelectric control

The movement classes used for myoelectric control were wrist supination and pronation, opening and closing of the hand and rest. These DoFs were selected since they can provide control of wrist rotation and hand aperture in a myoelectric prosthesis. The acquired EMG signals were filtered using a 2nd order Butterworth high-pass filter with 10 Hz cut-off to remove movement artefacts. For feature representation, spatial features designed by Donovan *et al* [46], namely, scaled mean absolute value, correlation coefficient, normalized mean absolute difference, and scaled raw mean absolute difference, were extracted along with the waveform length, hence five features per channel [47]. The features were extracted in windows of 200 ms with a 50% overlap to obtain fast update time, while preserving good classification accuracy [48].

Training data were acquired by asking the subjects to track a trapezoidal trajectory comprised of 3 s incline time, 5 s plateau and 3 s decline. The cursor moved horizontally with time while the vertical position was adjusted by the subject's contraction intensity. The plateaus of the trapezoidal profiles were at 40%, 50% and 70% of a prolonged maximum voluntary contraction (15 s). The three trajectories were tracked by the subjects for each movement class [49]. A 15 s recording of rest was acquired at the end.

The extracted features were used to train a sequential proportional control system. For sequential control, a linear discriminant analysis (LDA) classifier was trained and for proportional control, multiple linear regression models were used, one per movement class. This configuration was chosen because it is commonly applied for myoelectric control in the literature [50–55]. The LDA classifier can be trained fast, while still yielding robust control [52]. Linear discriminant analysis models the feature distribution within each class using a Gaussian distribution, assuming that all classes share the same covariance matrix. To classify a test sample, the posterior probabilities are computed by using Bayes' rule, and the class with the highest posterior probability is the output of the classifier, as explained in [56]. The multiple linear regression model fitted for the

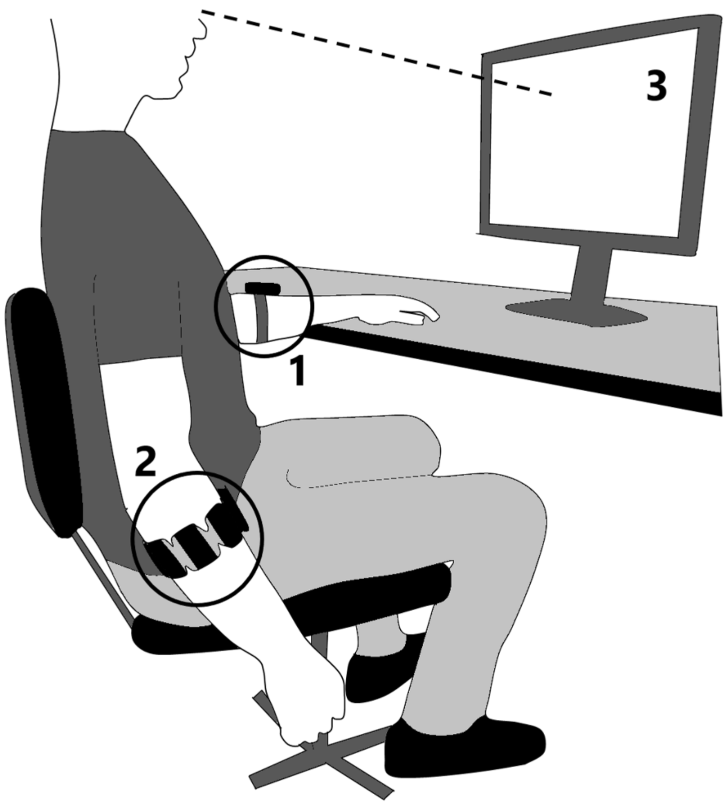

Figure 1. Illustration of the experimental setup: 1) the stimulation system with the electrode array (see figure 2) wrapped circumferentially around the non-dominant forearm and a stimulator placed on the dorsal side connected to a computer via USB; 2) the Myo armband placed on the dominant forearm to record EMG; and 3) the computer screen displaying the tasks to be performed in the experiment.

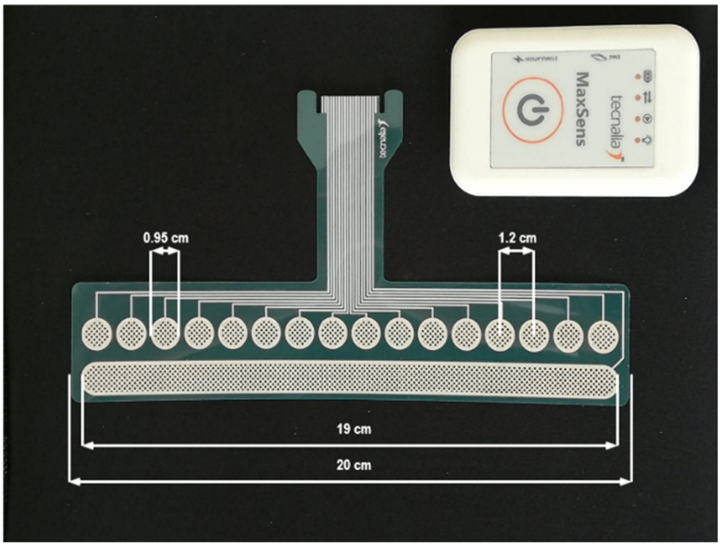

Figure 2. The 16-pad electrode array and the MaxSens stimulator. The electrode consisted of 16 circular active pads and a common reference pad.

decided movement class provided the proportional control output. The input of the regression model was a vector of mean absolute values calculated from a single window in each EMG channel. The output was the normalized level of muscle activation within the selected movement class.

The control of a two-DoF prosthesis was simulated by a planar cursor control task similarly to previous work [35]. The output of the myoelectric controller was a recognized movement class and a normalized value of the intensity of muscle contraction. The detected class determined the movement direction of the cursor (figure 3). Performing supination, pronation, opening and closing moved the cursor to the right, left, upwards, and downwards along the plane, respectively, while the estimated contraction intensity was mapped to the velocity of cursor movement. The cursor was controlled in velocity since this approach is used with commercial prostheses [57], where the muscle activation of the user is mapped into the velocity of prosthesis movement. The cursor initial position, as indicated in figure 3, represented a neutral prosthesis state, i.e. hand horizontal and fully open. Then, left and right movements of the cursor simulated wrist rotation into pronation and supination, while downwards and upwards movements corresponded to a decrease and increase in hand aperture, respectively. The maximum velocity of the cursor was adjusted so that a full range of each DoF could be traversed in 2 s. This corresponds to a maximum velocity of opening and closing in a Bebionic (RSL Steeper, United Kingdom) prosthesis [58]. The cursor moved smoothly within the plane; however, the plane was divided by a grid to indicate that the electrotactile feedback on the cursor position was in fact discrete, as explained in *2.3*. Each field of the grid corresponded to a unique combination of levels of wrist rotation and hand aperture.

2.3. Feedback configurations

Two coding schemes were designed to transmit wrist rotation and hand aperture information. As in previous studies a discrete coding strategy was adopted for both schemes [7, 32, 44, 59, 60]. Specifically, the full range of each feedback variable was divided into five intervals, as shown in figure 3.

2.3.1. Spatial configuration.

This feedback design was chosen in order to be intuitive for the subject, similar to what was initially proposed in [32]. The two proprioceptive feedback variables were coded by a spatially moving electrotactile stimulus. In addition, the movement of the stimulus mimicked direction of motion in the included DoFs. Wrist rotation was communicated by producing a stimulus that rotated around the forearm. Hand aperture was transmitted by moving two pads closer together as the hand closed and further apart during hand opening. The illustration of the spatial configuration can be seen in figure 4(d).

The pads were divided into two groups each responsible for conveying information about a single DoF. The dorsally placed pads were allocated for wrist rotation and the volar pads for hand aperture. The pads were furthermore paired such that each pair would represent one of the four intervals of the proprioceptive feedback variable. The absence of stimulation in all pad groups indicated the first interval, hence five in total. For wrist rotation, the pads were connected in side-by-side pairs. For right-handed subjects, the activation of the pairs of pads would rotate medially during supination and laterally during pronation. For hand aperture, the pairs consisted of oppositely located pads on the medial and lateral sides. When decreasing hand aperture, the active pads would move towards the volar side of the forearm and the distance between the pads would become shorter, and opposite for the increase. When both feedback variables were outside of the first interval (no stimulation), the pad pairs corresponding to the given level of hand aperture and rotation would be activated. Thus, a maximum of four pads could be active simultaneously. The reason for grouping adjacent pads to convey information about the rotational DoF was to improve sensation perception by stimulating a larger skin area, as in [25].

2.3.2. Amplitude configuration.

This is a simple coding scheme, in which the proprioceptive information is conveyed by increasing the current pulse amplitude. The advantage of this approach is that even more pads can be grouped together to stimulate a larger area of the skin, thereby eliciting clearer sensations. The feedback was provided in groups of four pads. An illustration of the amplitude-coding scheme can be seen in figure 4(a).

The dorsal area of the electrode was associated to wrist rotation and the volar to hand aperture, as in the spatial coding scheme. However, in the amplitude scheme, the decrease in the hand aperture was communicated by simultaneously increasing the pulse amplitude of the four volar pads through four levels plus no stimulation, hence five levels in total. The eight pads used for the wrist rotation were split such that the four medially placed pads communicated supination and four laterally placed indicated pronation. The amplitude of both groups could be changed through two levels, hence five levels in total, i.e. two pad groups times two levels plus no stimulation. The increasing amplitude corresponded to increased rotation in the respective direction. Since both DoFs were transmitted simultaneously, a maximum of eight pads could be active concurrently.

2.4. Experimental protocol

Thirteen able-bodied subjects (12 males and 1 female—12 right-handed and 1 left-handed with a mean age of 26.3 ± 2.3 years) were recruited. The subjects signed an informed consent form before commencing with the experiment. The experimental protocol was approved by the ethical committee of Region Nordjylland, Denmark (approval number N-20 150 075).

Each subject was introduced to each feedback configuration, trained to perceive and interpret the feedback, and finally performed an online myoelectric control task. The order of the feedback schemes was randomized across subjects. The duration of the experiment was approximately 2.5 h.

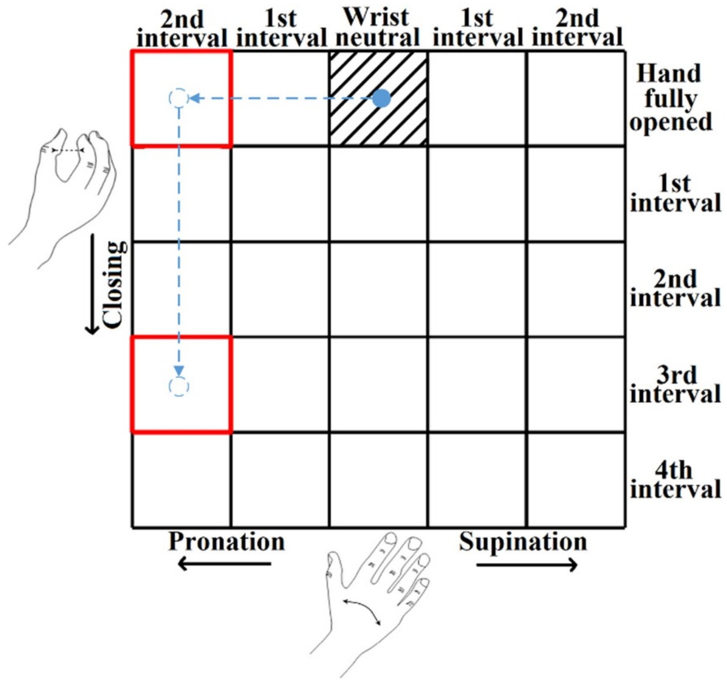

Figure 3. Illustration of the grid for the planar cursor control task and an example of two target cells. For the cursor (blue circle) to reach the target cell in first row and first column, pronation must be performed, and to reach the one in fourth row and first column, pronation followed by a decrease in hand aperture must be performed. The striped grid cell indicates a neutral position, i.e. a prosthesis, which is fully opened and with the palm in a horizontal position.

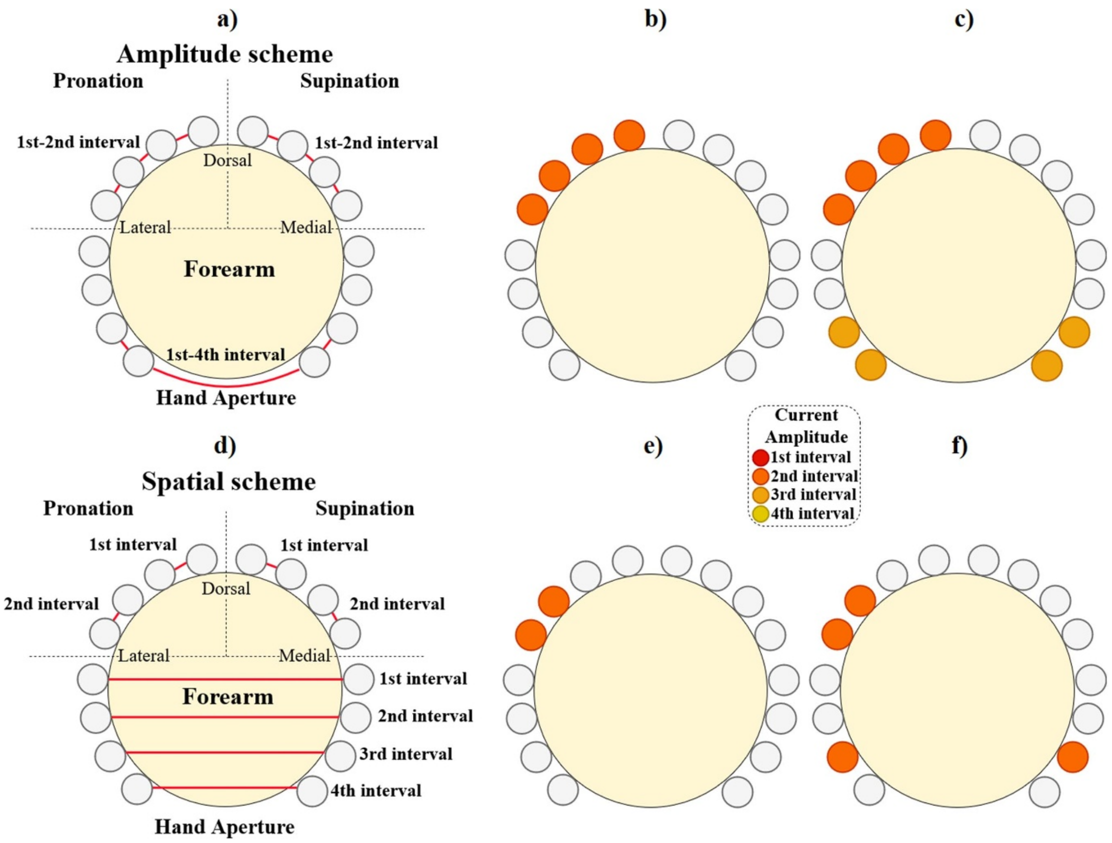

Figure 4. Illustration of the feedback schemes, (**a**) shows the amplitude coding and (**d**) shows the spatial coding. The red lines indicate which pads were coupled (see text). For the amplitude coding, the stimulation amplitude represented the position interval, whereas with spatial coding the position interval was communicated through location of active pads. The stimulation illustrated in (**b**) and (**e**) correspond to the position interval of the upper target cell in figure 3, for the amplitude and spatial coding, respectively, where (**c**) and (**f**) correspond to the lower target cell in figure 3.

First, the electrotactile and EMG recording systems were placed on the subject, as explained in *2.1*. Then, the training data for the myoelectric controller were collected, as described in *2.2*. Next, the subject practiced controlling the cursor movement using the myoelectric interface and visual feedback. It was crucial for the subject to achieve effective control since poor control could mask potential differences in performance between feedback configurations. The quality of closed-loop control was assessed by employing a target reaching task, which is a commonly used experimental paradigm to evaluate online myoelectric control [35–39]. The subject was presented with a grid shown in figure 3. The cursor was in the initial position. The subject training was divided into two runs of 3 min with a different visual feedback in each run. In the first run, the subject moved the cursor continuously and the current cursor position was shown on the screen. In the second run, the subject still moved the cursor in a continuous way; however, the visual feedback indicated only the cell of the grid currently containing the cursor. Therefore, the discretized visual feedback transmitted the same information as the electrotactile feedback that would be used later in the session.

After this brief training, the subject performed the target-reaching test using the discretized visual feedback. The task for the subject was to move the cursor from the initial position to the highlighted target position (grid cell highlighted in red) and dwell in that position for 1.5 s. The subject had 30 s to reach the target. This time was selected through pilot tests. The aim was to provide enough time so that the subjects were not pressured by the timer while still limiting the total duration of the experiment, as well as mental and physical fatigue due to continuous control. If the target was reached successfully, or the time limit expired (trial unsuccessful), the cursor would reset to neutral position and a new trial began. The grid cells were selected as targets in a random order and the test was finished when all the grid cells had been highlighted, hence 24 targets. If the subject did not achieve a completion rate $> 90\%$ and a mean time to reach the target < 10 s, the control was deemed ineffective and the subject was excluded. To reach the cells in the first row and third column (hereafter, single DoF targets), the subject would ideally move along a single DoF, and for the other cells, the subject needed to adjust both DoFs (hereafter, combined DoFs targets).

Next, four distinguishable stimulation levels were determined for each electrode pad. The stimulation levels were determined by changing amplitude while the pulse width and frequency were constant and set to 500 μs and 50 Hz, respectively.

To determine the stimulation levels the ascending method of limits [61] was applied to assess the sensation and discomfort thresholds. For the sensation threshold, the amplitude was set to 0 μA and increased in steps of 100 μA until the subject reported that he/she felt the sensation. For the discomfort threshold, the amplitude was initialized at the sensation threshold and increased in steps of 200 μA until the subject reported the stimulation as uncomfortable. First, the sensation thresholds were determined for all pads and then the amplitude values were fine-tuned by comparing the sensation intensity in neighboring pads. The goal was to achieve similar sensations across pads. The resulting amplitude was adopted as the first stimulation level. The same was then done for the discomfort threshold, and the resulting amplitude was adopted as the fourth stimulation level. The second and third stimulation levels were determined as the values that equidistantly divide the range between the first and fourth level.

In the spatial-coding scheme, all electrode pads were activated at the second level of stimulation intensity. The second intensity level was used to ensure that the stimulation elicited a sensation that could be clearly perceived by the subjects. This intensity was well above the detection threshold and still below the discomfort threshold. In the amplitude-coding scheme, the aperture pad group was activated at all four intensity levels, and the two wrist rotation groups were activated at the second and third level of stimulation intensity.

Following the psychometrics test, the subject was trained in understanding the sensory feedback schemes. The feedback schemes were first explained to the subject verbally. The sensory feedback training was divided into two phases: familiarization and reinforced learning. The familiarization phase provided the subjects with a short introduction to the scheme. The cursor was visualized and moved by the experimenter from the neutral position to a designated target cell. At the same time, the subject received electrotactile feedback on the cursor position. Therefore, the subject could associate visual feedback (the currently highlighted grid cell) to the electrotactile feedback that was delivered. The experimenter visited the grid cells along the row and column containing the neutral state, which corresponded to moving along a single DoF. This was deemed most important, since it was assumed that the subject will be able to recognize simultaneous feedback if he/she understands each DoF individually.

In the reinforced learning phase, the subject was asked to look away from the screen. The experimenter moved the cursor to a designated target cell and the subject was asked to report the grid cell solely by focusing on the electrotactile feedback. If the subject answered correctly, the cursor was reset to the neutral position and then moved to a new grid cell. If the subject answered incorrectly, the experimenter would indicate the correct cell verbally. Every cell of the grid was presented as the target once, by moving the cursor along the optimal path (the cursor was moved fully in one DoF and then in the other). However, the order of the DoFs was varied to avoid biasing the subject.

When all 24 cells were trained, the subject was given a short break before repeating the reinforced learning. The order of the target cells and DoFs was changed in the second run. The subject was given 2 min rest between the runs to avoid sensory adaptation.

Until this point, the subject trained the cursor control and sensory feedback separately. Both components were finally combined in the last phase of the experimental session, where online closed-loop control was assessed.

The subject was given a 3 min training period to be reacquainted with the myoelectric control and to further train the understanding of the feedback scheme. After a 2 min break, the subject performed a target-reaching test identical to that used with the visual feedback at the beginning of the session (target cell indicated by red color). However, this time the visual feedback on the cursor position was removed. Therefore, the subject had to estimate the cursor position solely by relying on the electrotactile feedback. The target-reaching test was performed two times with all cells of the grid as targets (24 repetitions) and there were 2 min of rest in between the two tests.

In order to preliminary assess the subjects' preference regarding the coding schemes, they were asked two questions at the end of the experiment: 1) whether they found the coding schemes intuitive to understand, and 2) which coding scheme, amplitude or spatial, they favored (if any).

2.5. Data analysis

The outcome measures were the number of successfully reached targets expressed in percent (completion rate), time to reach the target, distance error and path efficiency. These measures are commonly used in literature to evaluate the quality of control in target reaching tasks [35, 36]. Ideally, the subjects would be able to employ the closed-loop interface (myoelectric control and electrotactile feedback) to navigate the cursor from the initial to the target cell (configure the prosthesis DoFs) in minimum time and using the shortest path. Importantly, only successful trials were considered when computing the time to reach the target and path efficiency. Unsuccessful trials in which the 30 s timer has expired before the target was reached were excluded from this analysis. They were instead used to compute the distance error. The time to reach the target was measured from the start of a successful trial until the target was reached, including the dwell time. Path efficiency was computed by dividing the length of the shortest path from the initial position to the target with the length of the path that was actually traversed during online control. For single DoF targets, the shortest path was the distance in a straight line from the initial position to the border of the target, and for combined DoF targets, it was the distance to the target corner closest to the initial position. The distance error was calculated as the number of grid cells between the cursor and the target cell at the end of a trial. For instance, if the cursor was inside the target when surpassing the time limit, the distance was 0. If the cursor reached an adjacent grid cell directly above, below, left or right from the target, the distance was set to 1, and if the cursor ended up in an adjacent cell placed diagonally to the target, the distance was set to 2. This considered that the myoelectric control was sequential and the subjects could therefore move only in horizontal and vertical direction, hence, two cells would need to be traversed before reaching the target. The maximum score was 8, for instance, if the end-point was in the top left grid cell when the target was the bottom right grid cell. The outcome measures were computed for each trial and then averaged across all trials of a single subject in each feedback condition. The outcome measures computed for the online control with the visual feedback were used as the benchmark. Since the data were not normally distributed based on one-sample Kolmogorov–Smirnov tests, comparisons were made using non-parametric statistics. For the completion rate, time to reach the target and path efficiency, the Friedman test was used to assess if there was a statistically significant difference between the feedback modalities, and Tukey's honestly significant difference test was used for post-hoc pairwise comparisons. As the control with the visual feedback resulted in only three unsuccessful trials overall, the distance error was not evaluated in this condition. The distance error achieved with the spatial and amplitude feedback was compared using Wilcoxon signed-rank test. A significance level was set at $p < 0.05$. The results in the text are reported as median/interquartile range (IQR).

3. Results

3.1. Representative trajectories

Figure 5. shows examples of trajectories generated by subjects using spatial feedback to reach a target (red square) corresponding to a combined movement along both DoFs.

The cyan dashed lines demonstrate very good performance, while the blue dashed line is an example of a detour from the ideal path. The former trajectories indicate that the subjects successfully used the feedback to reach the target via a short route, i.e. the sequential movements along both DoFs were of appropriate magnitude. The two traces illustrate that the subjects could chose to move along the DoFs in a different order, that is, first adjust wrist rotation and then hand aperture, or vice versa. In this example, the subjects achieved a high performance in both cases, namely, a completion time of 7 s and 5.5 s, respectively, and a path efficiency of 74% and 70%, respectively. In the example with a detour, however, the subject misinterpreted the hand aperture interval before performing supination. When reaching the correct supination interval, the subject moved to a

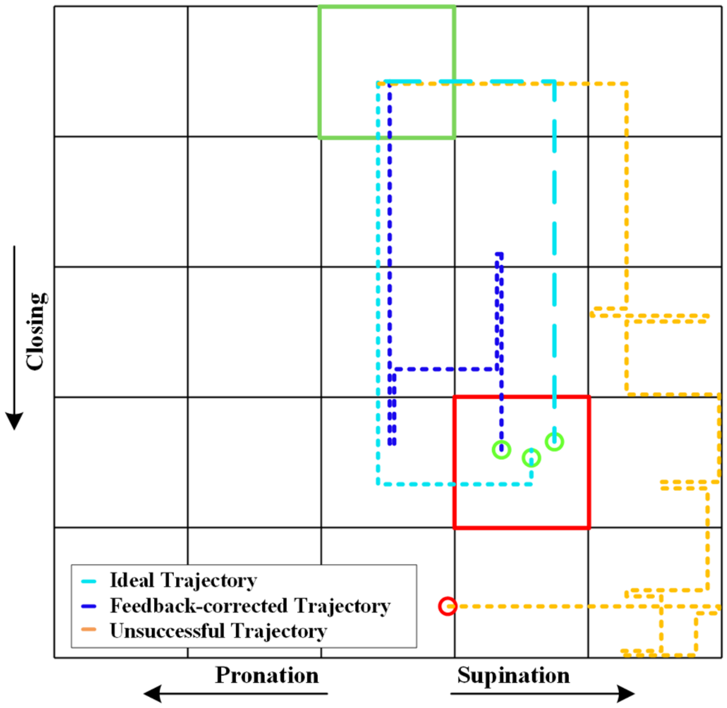

Figure 5. Examples of cursor trajectories when reaching a combined DoF target (red box) in the target-reaching test. The green and red box indicate the starting and target cell, respectively. The cyan dashed lines are examples of very good performance and the blue dashed line is a trajectory with several feedback-driven corrections. The orange trajectory is an example of an unsuccessful attempt at reaching the target. The green and red circles are end positions, indicating whether a particular trial was successful or not, respectively.

lower hand aperture before realizing the error and moving to the correct aperture. Therefore, the subject utilized the feedback to detect an erroneous level of a feedback variable and correct the cursor position accordingly. In this case, the completion time was 16 s and the path efficiency 46%. The orange dashed line demonstrates an unsuccessful trial. The subject initially overshot the target supination interval and then moved into higher hand aperture intervals. Finally, he/she moved towards the correct supination but did not successfully correct the hand aperture, thereby failing to reach the target (30 s timer expired). In this example, the path efficiency was 20% and the distance error was two cells.

3.2. Summary outcome measures

The success rate (median/IQR) in estimating the grid cell using electrotactile feedback in the reinforced learning phase was 75/22% and 79/14% using spatial and amplitude coding, respectively, with no significant difference between the two feedback schemes. The summary results for the quality of online control using three feedback modalities are shown in figure 6. Overall, only 7% of trials were unsuccessful. The median completion rate for the amplitude coding was not significantly different to that of the spatial coding. Importantly, the performance was high with both feedback configurations, with the median completion rates of more than 90% (94/10% for spatial and 94/2% for amplitude coding). Similarly, no significant difference was found in the time to reach the target (9/2 s for spatial and 10/3 s for amplitude), path efficiency (51/10% for spatial and 47/14% for amplitude) and distance error (2.5/1.9 grid cells from the target for spatial and 2/1.4 grid cells from the target for amplitude). Nevertheless, the mean completion rate and the time to reach the target were less variable across subjects when using amplitude coding. The amplitude condition was favored by 8 out of 13 subjects. However, most subjects struggled in choosing a favored feedback scheme as they found that both configurations were intuitive to understand. Accordingly, there was little difference in the completion rates across the preferred and non-preferred scheme (subjects preferring amplitude coding: 94/14% for spatial and 94/3% for amplitude; subjects preferring spatial coding: 90/9% for spatial and 96/7% for amplitude). As expected, the visual feedback outperformed both electrotactile feedback schemes. Almost all subjects reached all targets when using visual feedback and they were substantially faster compared to online control with electrotactile feedback. Interestingly, the path efficiency for electrotactile feedback was similar to that of the visual feedback.

3.3. Completion rates for individual targets

Figure 7. shows the completion rate for all targets individually. In both feedback schemes, the subjects were more successful in reaching the peripheral targets located along the edges of the grid, i.e. first and last row and column. In these targets, one or even

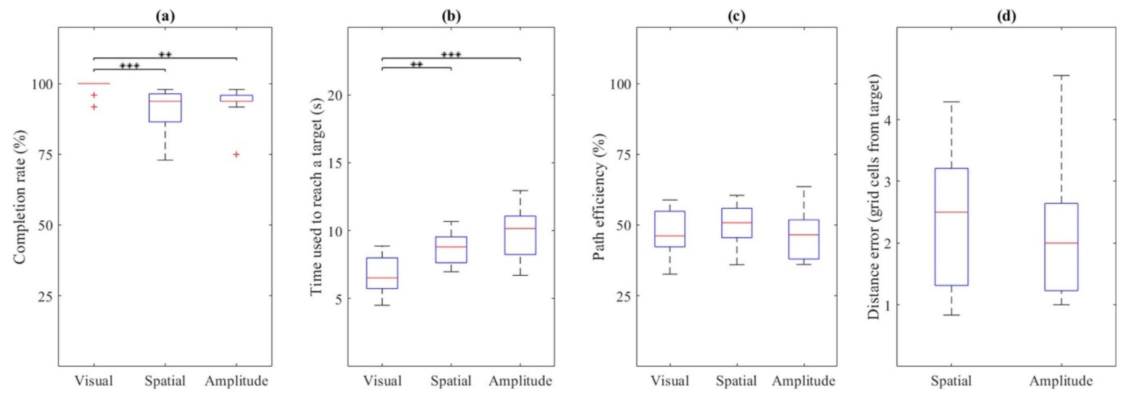

Figure 6. Box plots of the outcome measures extracted from the target-reaching tests using visual, spatial and amplitude feedback: (**a**) the completion rate, (**b**) the time used to reach a target, (**c**) the path efficiency and (**d**) the distance error. The red line, blue box, and black whiskers indicate the median, interquartile range and maximum and minimum values, while the red crosses are outliers. The asterisks indicate a p-value (*, $p < 0.05$; **, $p < 0.01$; ***, $p < 0.001$).

both (corner cells) of the DoFs are close to the limits of their range of motion, and this includes both single-DoF targets (first row cells, bottom cell in the third column) and the combined-DoFs targets (all other peripheral cells). And indeed, the completion rate (median/IQR) for the non-peripheral targets was 80/11% with spatial feedback and 89/5% with amplitude feedback, whereas the median completion rate for the peripheral targets was 96/2% with spatial feedback and 96/7% with amplitude feedback. The likely reason is that in the peripheral targets, the unintended myoelectric commands would not move the cursor outside of the cell due to the limits in the range of motion (as in a real prosthesis). Therefore, the subjects did not need to achieve an ideal rest state, while in the non-peripheral targets an unstable rest could lead to a cursor drifting outside of the cell during the dwell time. In addition, to reach a peripheral target, the subjects could rely on a simple control strategy where they would simply saturate the DoF in the direction of the peripheral cell.

The same reason is likely responsible for the fact that in both schemes a higher completion rate was achieved for the rotational single DoF targets (98/4% with spatial and 98/6% with amplitude coding) compared to the hand aperture single DoF targets (90/15% for spatial and 90/8% with amplitude coding). While moving along rotational DoF (first row), the hand aperture DoF is at the limit of the range of motion (the hand is fully open), whereas while closing the hand (third column), the wrist can be rotated both to the left and to the right.

The overall lowest completion rate (a cell with 62%) for spatial coding was worse compared to those of the amplitude coding (a cell with 85%).

4. Discussion

A compact multichannel electrotactile system was used to develop two electrotactile feedback schemes using spatial and amplitude coding to provide proprioceptive feedback about two DoFs simultaneously. The schemes were tested in able-bodied subjects using sequential proportional myoelectric control to perform a target-reaching task with a velocity-controlled cursor (simulating prosthesis operation). A discrete electrotactile feedback provided 9 intervals along single DoFs and 16 combinations of intervals along 2 DoFs.

The results demonstrated that a very good performance was achieved with both feedback-coding schemes. The average completion rates were high and the path efficiency in the electrotactile conditions was not significantly different to that achieved with visual feedback (benchmark). Even when the subjects were not able to navigate successfully to the target cell, they still ended up in the vicinity of the target (median distance error ∼2 cells out of max distance of 8 cells). The subjects were therefore able to correctly perceive and interpret two independent channels of electrotactile stimulation, despite they were delivered simultaneously and through a compact interface with closely spaced pads. In addition, the patterns of stimulation were substantially different between the two schemes (amplitude change versus movement across the skin), but nevertheless, the subjects could exploit both configurations successfully during the online control.

Our initial hypothesis was that spatial coding would lead to better performance and user experience, since it was assumed that this was a more intuitive interface, in which the movement of the electrotactile stimuli mimicked the movement of the controlled object (cursor/prosthesis). However, both feedback schemes resulted in similar performance in both the evaluation test and reinforced learning with a slight advantage of amplitude coding, which was characterized with less variability across subjects. Strictly speaking, the amplitude scheme also included a spatial code as the pronation and supination were

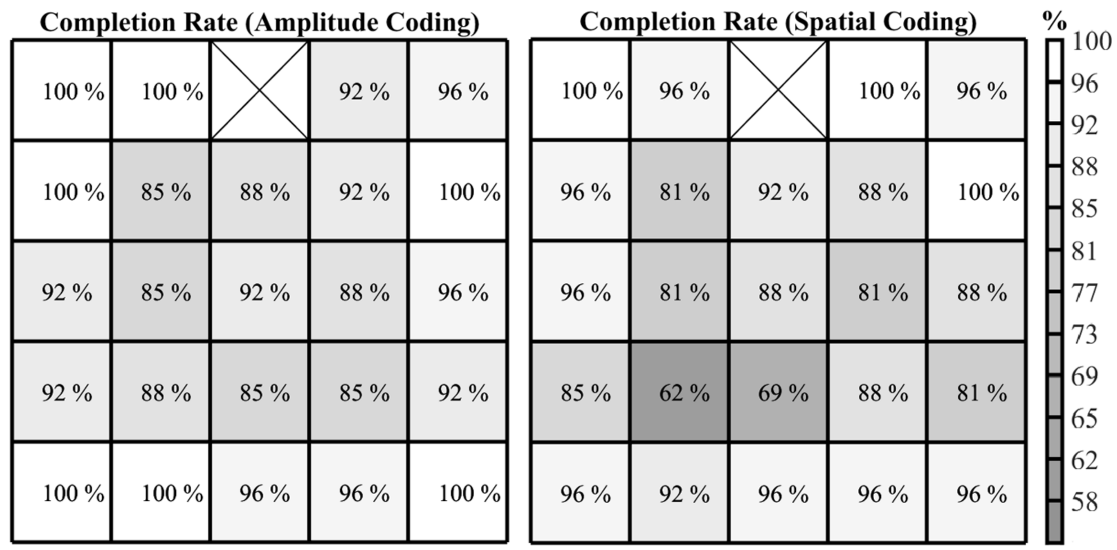

Figure 7. Completion rate for each target in the target-reaching tests using the amplitude and spatial coding, respectively.

communicated through separate pad groups. This had to be done so that the neutral position could be communicated as no stimulation. This could have contributed to a better consistency of the amplitude scheme across subjects.

The present study further emphasizes the advantage of a flexible system for electrotactile stimulation that is capable of implementing different coding schemes. A prospective user could test both amplitude and spatial modulation and select the scheme that feels better. In addition, some users might have a low tolerance to stimulation intensity (low dynamic range) and in this case, spatial modulation would be the only option. A similar coding scheme could be implemented using frequency instead of amplitude coding, but this could not be included in the present study due to technical constraints (frequency is a parameter common to all channels). An additional advantage of a flexible stimulation system is that it could be adjusted not only to the preference of the user but also to the characteristics of a specific prosthesis (multifunction versus dexterous device) or to the demands of a specific application (e.g. feedback in a lower limb prosthesis).

Importantly, the good performance in the present experiment was obtained after only a short training protocol (training time per scheme <30 min). It is likely that a longer training would lead to even higher completion rates, approaching the benchmark of visual feedback. The importance of training for the interpretation of tactile feedback has been demonstrated in [32] and [62]. However, as stated in [63], vision is dominant in learning motor control, and an equal performance should, therefore, not be expected.

An additional important conclusion from the present study is that the performance of closed-loop control is not determined only by the feedforward and feedback method, but also by the limitation and 'mechanical' interaction between the DoFs. The subjects were better in reaching states in which one of the DoFs was at the limit of the range of motion, and this benefited wrist rotation more than hand aperture.

Importantly, the times to reach the target were always well below the limit of 30 s, and this includes the pads with lower success rates placed centrally in the grid. Therefore, in the unsuccessful trials, the subjects likely failed not because they could not navigate to the correct pad (generate proper commands) but because they had difficulties to locate the cell by interpreting the feedback. In particular, two cells seemed to have been more challenging to find using spatial coding (figure 7, 62% and 69% success rates).

In general, it was a challenge to achieve a homogenous sensation during multi-site stimulation. This was especially apparent in the spatial scheme, where the sensation intensity was adjusted so that the elicited sensation was approximately identical in all pads. Some subjects reported difficulties in separating feedback variable levels, due to a notable difference in sensation intensity between them. The variation in the sensation intensity caused some feedback variable levels to be 'washed out' when receiving information regarding two DoFs simultaneously, as a stronger sensation would mask the weaker one. Allocating more time for the psychophysics stage of the experiment might have resulted in better discriminability between the levels. This was not possible in the present experiment due to time constraints, but it will be possible in the prospective clinical applications. A recent study has proposed a promising approach to decrease the time needed for the calibration of stimulation parameters [64].

One limitation of the study was that the stimulation electrodes were positioned on the contralateral arm with respect to the EMG recording. Even if this affected the closed-loop performance, which is unlikely, this is not relevant for the present study since the aim was to compare the relative performance of the two feedback schemes under the same conditions. Nevertheless, combining recording and stimulation into one device is required for clinical applications. Methods to minimize the interference have been proposed, such as, the use of concentric electrodes to minimize current leakage, time-division multiplexing [65], or artifact blanking and data segmentation [66]. Another limitation is the lack of amputee subjects and the fact that the myoelectric control did not involve a physical prosthesis. This, however, is unlikely to have affected the main aim of the study, which was the comparison of two different coding schemes via a compact stimulation system during closed-loop control. Specifically, an amputee subject might find it more difficult to accurately perceive the stimulation [32, 67], but this would likely affect both coding schemes in the same way. On the other hand, the presence of natural proprioception in the able-bodied subjects used in the study is unlikely to have provided an advantage in the test, since the cursor position was velocity-controlled and therefore could not be derived from wrist motions in a trivial way. Replacing the virtual interface (figure 3) with a real prosthesis would have introduced a movement delay, but this would also likely affect both coding schemes similarly.

The next step in this research would be to investigate the performance while increasing the resolution of the feedback scheme. The number of levels with the spatial feedback could be increased if the pads would be taken individually and not in pairs. With the amplitude feedback, more intensity levels could be considered in each group of pads. In this case, the device restrictions and subjects' sensory discrimination abilities are the only limit to the feedback resolution. Recognizing more levels would be more challenging for the subjects, especially during combined DoFs control. Therefore, a longer training would likely be necessary. Importantly, continuous feedback or a higher number of feedback intervals might not be more beneficial during daily life as high precision is often not necessary to accomplish functional tasks [59]. In addition, even though the feedback is discrete, the subjects could rely on internal models [68, 69] and/or incidental feedback [70] to estimate the levels in-between those which are explicitly provided by the feedback.

The psychometric properties of electrotactile stimulation were extensively investigated in literature [22], and this has been considered in the present study. The separation between the electrode pads (12 mm) was above the two-point spatial discrimination on the forearm (∼9 mm [71]). Similarly, since the feedback relied on only four, equidistantly arranged intensity levels, the separation between the levels was also well above the just noticeable difference in amplitude [72]. This ensured that the subjects would be able to detect the transition between adjacent electrode pads and amplitude levels. Previous studies investigating feedback used a similar number of location, amplitude and/or frequency levels, which were sometimes combined (mixed coding) to increase the feedback resolution [25, 32, 60, 73]. A specific challenge in the present study, however, was that the electrotactile codes corresponding to the two DoFs were simultaneously active, thereby possibly affecting the perception and interpretation [74]. Therefore, the previous results on optimal spatial and amplitude resolution for a single feedback variable could not be directly translated to a two-DoF scenario.

The four times four level coding schemes were selected based on pilot testing. Nevertheless, determining the optimal spatial and amplitude resolution when providing two feedback variables simultaneously is indeed an important future goal. Similarly, the coding could be extended to represent more feedback variables. For example, grasping force could be communicated by modulating the stimulation frequency of the hand aperture feedback [25]. This would allow communicating the full state of a multifunctional prosthesis, which is indeed an ultimate goal. The control was sequential in the present study since it was based on pattern classification. Therefore, although the subjects felt the sensations for two DoFs simultaneously, they could move only one DoF at a time. A relevant future step would be to evaluate the feedback schemes when using simultaneous control via regression [75].

5. Conclusion

This study investigated the effectiveness of two novel electrotactile feedback schemes using spatial and amplitude coding to communicate proprioceptive information about two DoFs simultaneously. The results of closed-loop myoelectric control showed that even with minimal training (<30 min) a very good performance can be achieved with both configurations. In addition, the subjects reported that both feedback schemes were easily comprehensible and intuitive. The stimulation interface used to implement the feedback is compact, and therefore, it could be easily integrated in a two DoF myoelectric prosthesis, potentially enhancing the prosthesis utility and embodiment in users.

Acknowledgments

The authors would like to thank the participants, who all participated voluntarily. This work has been supported by the projects 8022-00243A (ROBIN) and 8022-00226B funded by the Independent Research Fund Denmark and an EU funded project TACTILITY (H2020-ICT-25-856718).

ORCID iDs

Jakob L Dideriksen https://orcid.org/0000-0001-6587-0865
Strahinja Dosen https://orcid.org/0000-0003-3035-147X

References

[1] Schofield J S, Evans K R, Carey J P and Hebert J S 2014 Applications of sensory feedback in motorized upper extremity prosthesis: A review *Expert Rev. Med. Devices* **11** 499–511
[2] Østlie K, Magnus P, Skjeldal O H, Garfelt B and Tambs K 2011 Mental health and satisfaction with life among upper limb amputees: A Norwegian population-based survey comparing adult acquired major upper limb amputees with a control group *Disability Rehabil.* **33** 1594–607
[3] Geethanjali P 2016 Myoelectric control of prosthetic hands : state-of-the-art review *Med. Devices Evidence Res.* **9** 247–55
[4] Biddiss E A and Chau T T 2007 Upper limb prosthesis use and abandonment: A survey of the last 25 years *Prosthet. Orthot. Int.* **31** 236–57
[5] Cordella F, Ciancio A L, Sacchetti R, Davalli A, Cutti A G, Guglielmelli E and Zollo L 2016 Literature review on needs of upper limb prosthesis users *Front. Neurosci.* **10** 1–14
[6] Peerdeman B, Hermens H, Stramigioli S, Rietman H, Witteveen H, Huis in 't Veld R, Misra S, Veltink P and Boere D 2011 Myoelectric forearm prostheses: state of the art from a user-centered perspective *J. Rehabil. Res. Dev.* **48** 719–38
[7] Pamungkas D and Ward K 2015 Electro-tactile feedback system for a prosthetic hand. *22nd Annu. Int. Conf. Mechatronics Mach. Vis. Pract. M2VIP 2015* pp 27–38
[8] Jorgovanovic N, Dosen S, Djozic D J, Krajoski G and Farina D 2014 Virtual grasping: closed-loop force control using electrotactile feedback *Comput. Math. Methods Med.* **2014** 13
[9] Witteveen H J B B, Luft F, Rietman J S and Veltink P H 2014 Stiffness feedback for myoelectric forearm prostheses using vibrotactile stimulation *IEEE Trans. Neural Syst. Rehabil. Eng.* **22** 53–61
[10] Witteveen H J B, Rietman H S and Veltink P H 2015 Vibrotactile grasping force and hand aperture feedback for myoelectric forearm prosthesis users *Prosthet. Orthot. Int.* **39** 204–12
[11] Witteveen H J B B, Rietman J S and Veltink P H 2012 Grasping force and slip feedback through vibrotactile stimulation to be used in myoelectric forearm prostheses *2012 Proc. Annu. Int. Conf. IEEE Eng. Med. Biol. Soc. EMBS* pp 2969–72
[12] Clemente F, D'Alonzo M, Controzzi M, Edin B B and Cipriani C 2016 Non-invasive, temporally discrete feedback of object contact and release improves grasp control of closed-loop myoelectric transradial prostheses *IEEE Trans. Neural Syst. Rehabil. Eng.* **24** 1314–22
[13] Vincent Systems 2005 Vincent evolution 2 (Accessed 5 May 2020) https://vincentsystems.de/en/prosthetics/vincent-evolution-2/
[14] Antfolk C, D'Alonzo M, Rosén B, Lundborg G, Sebelius F, Cipriani C, Fredrik S and Cipriani C 2013 Sensory feedback in upper limb prosthetics *Expert Rev. Ltd.* **10** 45–54
[15] D'Anna E, Petrini F M, Artoni F, Popovic I, Simanić I, Raspopovic S and Micera S 2017 A somatotopic bidirectional hand prosthesis with transcutaneous electrical nerve stimulation based sensory feedback *Sci. Rep.* **7** 15
[16] Vargas L, Shin H, Huang H, Zhu Y and Hu X 2019 Object stiffness recognition using haptic feedback delivered through transcutaneous proximal nerve stimulation *J. Neural Eng.* **17** 016002
[17] Petrini F M *et al* 2019 Six-month assessment of a hand prosthesis with intraneural tactile feedback *Ann. Neurol.* **85** 137–54
[18] Clemente F *et al* 2019 Intraneural sensory feedback restores grip force control and motor coordination while using a prosthetic hand *J. Neural Eng.* **16** 026034
[19] Flesher S N, Collinger J L, Foldes S T, Weiss J M, Downey J E, Tyler-Kabara E C, Bensmaia S J, Schwartz A B, Boninger M L and Gaunt R A 2016 Intracortical microstimulation of human somatosensory cortex *Sci. Transl. Med.* **8** 361ra141
[20] Tabot G A, Dammann J F, Berg J A, Tenore F V, Boback J L, Vogelstein R J and Bensmaia S J 2013 Restoring the sense of touch with a prosthetic hand through a brain interface *Proc. Natl Acad. Sci.* **110** 18279–84
[21] Szeto A Y J and Saunders F A 1982 Electrocutaneous stimulation for sensory communication in rehabilitation engineering *IEEE Trans. Biomed. Eng.* **BME-29** 300–8
[22] Kaczmarek K A, Webster J G, Bach-y-rita P and Tompkins W J 1991 Electrotactile and vibrotactile displays for sensory substitution systems *IEEE Trans. Biomed. Eng.* **38** 1–16
[23] Franceschi M, Seminara L, Dosen S, Strbac M, Valle M and Farina D 2017 A system for electrotactile feedback using electronic skin and flexible matrix electrodes: experimental evaluation *IEEE Trans. Haptics* **10** 162–72
[24] Geng B, Yoshida K, Petrini L and Jensen W 2012 Evaluation of sensation evoked by electrocutaneous stimulation on forearm in nondisabled subjects *J. Rehabil. Res. Dev.* **49** 297
[25] Dosen S *et al* 2016 Multichannel electrotactile feedback with spatial and mixed coding for closed-loop control of grasping force in hand prostheses *IEEE Trans. Neural Syst. Rehabil. Eng.* **25** 183–95
[26] Svensson P, Wijk U, Björkman A and Antfolk C 2017 A review of invasive and non-invasive sensory feedback in upper limb prostheses *Expert Rev. Med. Devices* **14** 439–47
[27] Ingram H A, van Donkelaar P, Cole J, Vercher J L, Gauthier G M and Miall R C 2000 The role of proprioception and attention in a visuomotor adaptation task *Exp. Brain Res.* **132** 114–26
[28] Schiefer M A, Graczyk E L, Sidik S M, Tan D W and Tyler D J 2018 Artificial tactile and proprioceptive feedback improves performance and confidence on object identification tasks *PLoS One* **13** 1–18
[29] Horch K, Meek S, Taylor T G and Hutchinson D T 2011 Object discrimination with an artificial hand using electrical stimulation of peripheral tactile and proprioceptive pathways with intrafascicular electrodes *IEEE Trans. Neural Syst. Rehabil. Eng.* **19** 483–9
[30] Erwin A and Sup F C 2015 A haptic feedback scheme to accurately position a virtual wrist prosthesis using a three-node tactor array ed S J Bensmaia *PLoS One* **10** e0134095
[31] Battaglia E, Clark J, Bianchi M, Catalano M, Bicchi A and O'Malley M K 2019 Skin stretch haptic feedback to convey closure information in anthropomorphic, under-actuated upper limb soft prostheses *IEEE Trans. Haptics* **12** 508–20
[32] Štrbac M *et al* 2016 Integrated and flexible multichannel interface for electrotactile stimulation *J. Neural Eng.* **13** 1–16
[33] Arakeri T J, Hasse B A and Fuglevand A J 2018 Object discrimination using electrotactile feedback *J. Neural Eng.* **15** 046007
[34] D'Anna E *et al* 2019 A closed-loop hand prosthesis with simultaneous intraneural tactile and position feedback *Sci. Robot.* **4** 13
[35] Scheme E J, Hudgins B S and Englehart K B 2013 Confidence-based rejection for improved pattern recognition myoelectric control *IEEE Trans. Biomed. Eng.* **60** 1563–70
[36] Scheme E and Englehart K 2013 Validation of a selective ensemble-based classification scheme for myoelectric control

using a three dimensional Fitts' law test *Neural Syst. Rehabil. Eng. IEEE Trans.* **21** 616–23
[37] Wurth S M and Hargrove L J 2014 A real-time comparison between direct control, sequential pattern recognition control and simultaneous pattern recognition control using a Fitts' law style assessment procedure *J. Neuroeng. Rehabil.* **11** 1–13
[38] Kamavuako E N, Scheme E J and Englehart K B 2014 On the usability of intramuscular EMG for prosthetic control: A Fitts' Law approach *J. Electromyogr. Kinesiol.* **24** 770–7
[39] Waris A, Mendez I, Englehart K, Jensen W and Kamavuako E N 2019 On the robustness of real-time myoelectric control investigations: A multiday Fitts' law approach *J. Neural Eng.* **16** 026003
[40] Mendez I, Hansen B W, Grabow C M, Smedegaard E J L, Skogberg N B, Uth X J, Bruhn A, Geng B and Kamavuako E N 2017 Evaluation of the Myo Armband for the classification of hand motions *Int. Conf. Rehabil. Robot.* **15** 1211–4
[41] Visconti P, Gaetani F, Zappatore G A and Primiceri P 2018 Technical features and functionalities of Myo armband: an overview on related literature and advanced applications of myoelectric armbands mainly focused on arm prostheses *Int. J. Smart Sens. Intell. Syst.* **11** 1–25
[42] Strbac M *et al* 2017 Short-and long-term learning of feedforward control of a myoelectric prosthesis with sensory feedback by amputees *IEEE Trans. Neural Syst. Rehabil. Eng.* **25** 2133–45
[43] Witteveen H J B, Droog E A, Rietman J S and Veltink P H 2012 Vibro- and electrotactile user feedback on hand opening for myoelectric forearm prostheses *IEEE Trans. Biomed. Eng.* **59** 2219–26
[44] Isaković M, Belić M, Došen S, Štrbac M, Popović I, Keller T and Farina D 2016 Electrotactile feedback improves performance and facilitates learning in the routine grasping task *Eur. J. Transl. Myol.* **26** 197–202
[45] Patel G K, Dosen S, Castellini C and Farina D 2016 Multichannel electrotactile feedback for simultaneous and proportional myoelectric control *J. Neural Eng.* **13** 056015
[46] Donovan I M, Puchin J, Okada K and Zhang X 2017 Simple space-domain features for low-resolution sEMG pattern recognition *39th Ann. Int. Conf. IEEE Eng. Med. Biol. Soc. EMBS* pp 62–65
[47] Hudgins B, Parker P and Scott R N 1993 A new strategy for multifunction myoelectri control *IEEE Trans. Biomed. Eng.* **40** 82–94
[48] Menon R, Lakany H, Di Caterina G, Conway B A, Petropoulakis L and Soraghan J J 2017 Study on interaction between temporal and spatial information in classification of emg signals for myoelectric prostheses *IEEE Trans. Neural Syst. Rehabil. Eng.* **25** 1832–42
[49] Celadon N, Do S, Binder I, Ariano P and Farina D 2016 Proportional estimation of finger movements from high-density surface electromyography *J. Neuroeng. Rehabil.* **13** 1–19
[50] Scheme E and Englehart K 2011 Electromyogram pattern recognition for control of powered upper-limb prostheses: state of the art and challenges for clinical use *J. Rehabil. Res. Dev.* **48** 643–60
[51] Yang D, Gu Y, Thakor N V and Liu H 2019 Improving the functionality, robustness, and adaptability of myoelectric control for dexterous motion restoration *Exp. Brain Res.* **237** 291–311
[52] Englehart K and Hudgins B 2003 A robust, real-time control scheme for multifunction myoelectric control *IEEE Trans. Biomed. Eng.* **50** 848–54
[53] Powell M A, Kaliki R R and Thakor N V 2014 User training for pattern recognition-based myoelectric prostheses: improving phantom limb movement consistency and distinguishability *IEEE Trans. Neural Syst. Rehabil. Eng.* **22** 522–32
[54] Simon A M, Hargrove L J, Lock B A and Kuiken T A 2011 The target achievement control test: evaluating real-time myoelectric pattern recognition control of a multifunctional upper-limb prosthesis *J. Rehabil. Res. Dev.* **48** 619–27
[55] Parker P, Englehart K and Hudgins B 2006 Myoelectric signal processing for control of powered limb prostheses *J. Electromyogr. Kinesiol.* **16** 541–8
[56] Duda R O, Hart P E and Stork D G 2001 *Pattern Classification* (New York: Wiley)
[57] Fougner A, Stavdahl O, Kyberd P J, Losier Y G and Parker P A 2012 Control of upper limb prostheses: terminology and proportional myoelectric controla review *IEEE Trans. Neural Syst. Rehabil. Eng.* **20** 663–77
[58] Belter J T, Segil J L, Dollar A M and Weir R F 2013 Mechanical design and performance specifications of anthropomorphic prosthetic hands: a review *J. Rehabil. Res. Dev.* **50** 599–618
[59] Cipriani C, Segil J L, Clemente F, Richard R F and Edin B 2014 Humans can integrate feedback of discrete events in their sensorimotor control of a robotic hand *Exp. Brain Res.* **232** 3421–9
[60] Schweisfurth M A, Markovic M, Dosen S, Teich F, Graimann B and Farina D 2016 Electrotactile EMG feedback improves the control of prosthesis grasping force *J. Neural Eng.* **13** 056010
[61] Kingdom A A and Prins N 2009 *Psychophysics: A Practical Introduction* (New York: Academic Press)
[62] Štrbac M, Isaković M, Belić M, Popović I, Simanić I, Farina D, Keller T and Došen S 2017 Short-and long-term learning of feedforward control of a myoelectric prosthesis with sensory feedback by amputees *IEEE Trans. Neural Syst. Rehabil. Eng.* **25** 2133–45
[63] Adams J A, Gopher D and Lintern G 1977 Effects of visual and proprioceptive feedback on motor learning *J. Mot. Behav.* **9** 11–22
[64] Isakovic M, Malešević J, Keller T, Kostić M and Štrbac M 2019 Optimization of semiautomated calibration algorithm of multichannel electrotactile feedback for myoelectric hand prosthesis *Appl. Bionics Biomech.* **2019** 9298758
[65] Dosen S, Schaeffer M and Farina D 2014 Time-division multiplexing for myoelectric closed-loop control using electrotactile feedback *J. Neuroeng. Rehabil.* **11** 1–10
[66] Hartmann C, Došen S, Amsuess S and Farina D 2015 Closed-loop control of myoelectric prostheses with electrotactile feedback: influence of stimulation artifact and blanking *IEEE Trans. Neural Syst. Rehabil. Eng.* **23** 807–16
[67] Chai G, Sui X, Li S, He L and Lan N 2015 Characterization of evoked tactile sensation in forearm amputees with transcutaneous electrical nerve stimulation *J. Neural Eng.* **12** 066002
[68] Saunders I and Vijayakumar S 2011 The role of feed-forward and feedback processes for closed-loop prosthesis control *J. Neuroeng. Rehabil.* **8** 60
[69] Markovic M, Schweisfurth M A, Engels L F, Farina D and Dosen S 2018 Myocontrol is closed-loop control: incidental feedback is sufficient for scaling the prosthesis force in routine grasping *J. Neuroeng. Rehabil.* **15** 11
[70] Wilke M A, Niethammer C, Meyer B, Farina D and Dosen S 2019 Psychometric characterization of incidental feedback sources during grasping with a hand prosthesis *J. Neuroeng. Rehabil.* **16** 13
[71] Solomonow M, Lyman J and Freedy A 1977 Electrotactile two-point discrimination as a function of frequency, body site, laterality, and stimulation codes *Ann. Biomed. Eng.* **5** 47–60
[72] Dong J, Kamavuako E N, Dosen S, Jensen W and Geng B 2020 The short-term repeatability of subdermal electrical stimulation for sensory feedback *IEEE Access* **8** 63983–92

[73] Anani A B, Ikeda K and Körner L M 1977 Human ability to discriminate various parameters in afferent electrical nerve stimulation with particular reference to prostheses sensory feedback *Med. Biol. Eng. Comput.* **15** 363–73

[74] Geng B, Yoshida K and Jensen W 2011 Impacts of selected stimulation patterns on the perception threshold in electrocutaneous stimulation *J. Neuroeng. Rehabil.* **8** 9

[75] Hahne J M, Markovic M and Farina D 2017 User adaptation in myoelectric man-machine interfaces *Sci. Rep.* **7** 1–10